The Regional Ocean Modeling System: New Time-stepping Algorithms to Reduce Mode-splitting Error and to Ensure Constancy Preservation

D. B. Haidvogel[1], A. F. Shchepetkin[2], and H. G. Arango[1]

[1]*Institute of Marine and Coastal Sciences, Rutgers University*
71 Dudley Road, New Brunswick, NJ 08901 USA
dale@imcs.rutgers.edu

[2]*Institute of Geophysics and Planetary Physics, UCLA*
405 Hilgard Avenue, Los Angeles, CA 90095 USA
alex@atmos.ucla.edu

1 Introduction

ROMS is a versatile, state-of-the-art, free-surface, hydrostatic primitive equation ocean circulation model developed at Rutgers University and UCLA. As its predecessors, ROMS is terrain-following, and is discretized in space on an orthogonal curvilinear, Arakawa C-grid. System attributes include extensive restructuring for sustained performance on parallel-computing platforms (using MPI or openMP); high-order, weakly dissipative algorithms for tracer advection; a unified treatment of surface and bottom boundary layers; an integrated set of procedures for data assimilation (e.g., optimal interpolation, reduced-state Kalman filter, and adjoint-based methods); advanced treatments of open boundary conditions; and redesigned mode-splitting and split-explicit time-stepping algorithms with enhanced robustness and conservation properties. Below, we provide a condensed discussion of the last of these algorithmic improvements, distilled from Shcheptekin and McWilliams (2004). More complete descriptions of all of the above features can be found in this reference, and in Marchesiello et al. (2001), Moore et al. (2005), Shchepetkin and McWilliams (1998, 2003), Warner et al. (2005), and on the ROMS web site (http://marine.rutgers.edu/po/index.php?model=roms).

The remaining sections are organized as follows. Section 2 briefly defines the terrain-following coordinate currently in use in ROMS. Section 3 describes two sources of potential error associated with the use of split-explicit time-stepping: loss of constancy peservation and mode-splitting error. Finally, section 4 describes the new split-explicit time-stepping scheme developed for use in ROMS to contend with these error sources.

2 ROMS generalized topography-following coordinate

In a topography-following vertical coordinate system there is a transformation,

$$z = z(x, y, \sigma), \tag{1}$$

where z is the Cartesian height and σ is the vertical distance from the surface measured as the fraction of the local water column thickness; *i.e.*, $-1 \le \sigma \le 0$, $\sigma = 0$ corresponds to the free surface, $z = \zeta$, and $\sigma = -1$ corresponds to the oceanic bottom, $z = -h(x,y)$. In the case of the classical σ-coordinate, (1) reduces to

$$z = \sigma \cdot h(x,y). \tag{2}$$

This may be combined with nonlinear stretching, $S(\sigma)$,

$$z(x,y,\sigma) = S(\sigma)\cdot h(x,y)\,. \tag{3}$$

and further generalized into the S-coordinate of Song and Haidvogel (1994) which in essence behaves like (2) in shallow regions and (3) in deep.

Discretization of the vertical coordinate introduces a set of coordinate surfaces,

$$\left\{ z_{k+\frac{1}{2}} = z_{k+\frac{1}{2}}(x,y)\,, \quad k=0,1,...,N \right\}, \tag{4}$$

where $z_{\frac{1}{2}} \equiv z^{(0)}_{\frac{1}{2}} \equiv -h$ and $z_{N+\frac{1}{2}} \equiv \zeta$. If the ocean is at rest, the free-surface elevation is $\zeta = 0$, hence $z_{N+\frac{1}{2}} = 0$. In the case of a non-zero ζ, all $z_{k+\frac{1}{2}}$ are displaced by a distance proportional to ζ and the distance from the bottom as the fraction of unperturbed local depth,

$$z_{k+\frac{1}{2}} = z^{(0)}_{k+\frac{1}{2}} + \zeta\left(1+\frac{z^{(0)}_{k+\frac{1}{2}}}{h}\right) \tag{5}$$

As a result the perturbed grid-box height, $\Delta z_k \equiv z_{k+\frac{1}{2}} - z_{k-\frac{1}{2}}$, is related to the unperturbed height, $\Delta z^{(0)}_k \equiv z^{(0)}_{k+\frac{1}{2}} - z^{(0)}_{k-\frac{1}{2}}$ according to

$$\Delta z_k = \Delta z^{(0)}_k \left(1+\frac{\zeta}{h}\right), \tag{6}$$

where the multiplier $(1+\zeta/h)$ is independent of the vertical coordinate. One consequence of (6) is the fact that vertical mass fluxes generated by a purely barotropic motion vanish identically at every interface, $z_{k+\frac{1}{2}}$.

3 Some issues regarding split-explicit time-stepping

3.1 Integral conservation and constancy preservation for tracers

Combining the tracer equation in advective form,

$$\frac{\partial q}{\partial t} + \left(\mathbf{u}\cdot\nabla\right) q = 0 \tag{7}$$

with the statement of nondivergence,

$$\left(\nabla\cdot\mathbf{u}\right) = 0\,, \tag{8}$$

the tracer equation in conservation form becomes

$$\frac{\partial q}{\partial t} + \nabla\cdot\left(\mathbf{u}q\right) = 0\,. \tag{9}$$

As a consequence of (7), if the tracer is specified as a spatially uniform field at the initial time, it remains so regardless of the velocity field. On the other hand, as a consequence of (9), the volume integral of the tracer concentration is conserved in the absence of incoming and outgoing fluxes across the domain boundary. The continuity equation (8) provides the compatibility condition between these two properties.

Consider the discretization of (9) obtained using a finite-volume approximation,

$$\begin{aligned}\Delta\mathscr{V}^{n+1}_{i,j,k}q^{n+1}_{i,j,k} = \Delta\mathscr{V}^{n}_{i,j,k}q^{n}_{i,j,k} - \Delta t \Big[&\widetilde{q}_{i+\frac{1}{2},j,k}U_{i+\frac{1}{2},j,k} - \widetilde{q}_{i-\frac{1}{2},j,k}U_{i-\frac{1}{2},j,k} \\ &+\widetilde{q}_{i,j+\frac{1}{2},k}V_{i,j+\frac{1}{2},k} - \widetilde{q}_{i,j-\frac{1}{2},k}V_{i,j-\frac{1}{2},k} \\ &+\widetilde{q}_{i,j,k+\frac{1}{2}}W_{i,j,k+\frac{1}{2}} - \widetilde{q}_{i,j,k-\frac{1}{2}}W_{i,j,k-\frac{1}{2}}\Big]\,,\end{aligned} \tag{10}$$

where $q_{i,j,k}$ is understood to be a volume-averaged concentration over the grid-box $\Delta\mathscr{V}_{i,j,k}$,

$$q_{i,j,k} = \frac{1}{\Delta\mathscr{V}^{n}_{i,j,k}} \int\limits_{\Delta\mathscr{V}^{n}_{i,j,k}} q\,\mathrm{d}\mathscr{V}\,. \tag{11}$$

The $\widetilde{q}_{i+\frac{1}{2},j,k}$ are the interfacial values of tracer concentration. $U_{i+\frac{1}{2},j,k}$, $V_{i,j+\frac{1}{2},k}$, and $W_{i,j,k+\frac{1}{2}}$ are volumetric fluxes in the two horizontal and vertical directions. These are defined as velocity components multiplied by the contact area between two adjacent grid boxes,

$$\begin{aligned}U_{i+\frac{1}{2},j,k} &= u_{i+\frac{1}{2},j,k}\Delta z_{i+\frac{1}{2},j,k}\Delta\eta_{i+\frac{1}{2},j} \\ V_{i,j+\frac{1}{2},k} &= v_{i,j+\frac{1}{2},k}\Delta z_{i,j+\frac{1}{2},k}\Delta\xi_{i,j+\frac{1}{2}}\,,\end{aligned} \tag{12}$$

where $\Delta z_{i+\frac{1}{2},j,k}$, $\Delta\eta_{i,j+\frac{1}{2}}$, and $\Delta z_{i,j+\frac{1}{2},k}$, $\Delta\xi_{i,j+\frac{1}{2}}$ are vertical and horizontal measures of the corresponding grid-box interfaces ($\Delta\xi\,,\Delta\eta$ may be non-uniform because of the curvilinear horizontal coordinates). The superscripts $n+1$ and n denote new and old time steps. The time step for the flux variables in (10) is not specified yet, but must be effectively at $n+{}^1/_2$ to achieve second-order temporal accuracy. However, the flux form by itself guarantees exact conservation of the global volume integral of the advected quantity as long as there is no net flux across the domain boundary.

Setting $q_{i,j,k} \equiv 1$ in (10) yields the discretized continuity equation,

$$\Delta\mathscr{V}^{n+1}_{i,j,k} = \Delta\mathscr{V}^{n}_{i,j,k} - \Delta t\cdot\Big[U_{i+\frac{1}{2},j,k} - U_{i-\frac{1}{2},j,k} + V_{i,j+\frac{1}{2},k} - V_{i,j-\frac{1}{2},k} + W_{i,j,k+\frac{1}{2}} - W_{i,j,k-\frac{1}{2}}\Big]\,. \tag{13}$$

Once it holds, the conservative form of the discrete tracer equation (10) also has the property of constancy preservation in addition to global content conservation.

In a hydrostatic model the discrete continuity equation (13) is needed to compute vertical velocity rather than grid-box volume $\Delta\mathscr{V}^{n+1}_{i,j,k}$. [The latter is entirely controlled by change of ζ via (6).] Hence,

$$W_{i,j,\frac{1}{2}} = 0\,, \qquad \text{at the sea floor, and} \tag{14}$$

$$W_{i,j,k+\frac{1}{2}} = -\sum_{k'=1}^{k}\left\{\frac{\Delta\mathscr{V}^{n+1}_{i,j,k'} - \Delta\mathscr{V}^{n}_{i,j,k'}}{\Delta t} + U_{i+\frac{1}{2},j,k'} - U_{i-\frac{1}{2},j,k'} + V_{i,j+\frac{1}{2},k'} - V_{i,j-\frac{1}{2},k'}\right\} \tag{15}$$

$$\text{for all} \qquad k = 1,2,...,N\,,$$

which, in fact, defines the meaning of $W_{i,j,k+\frac{1}{2}}$ as a finite-volume flux across the *moving* grid-box interface $z_{i,j,k+\frac{1}{2}}$. Vertical summation of (13) for different k leads to the equation for the free surface,

$$\zeta^{n+1}_{i,j} = \zeta^{n}_{i,j} - \frac{\Delta t}{\Delta\mathscr{A}_{i,j}}\Big[\overline{U}_{i+\frac{1}{2},j} - \overline{U}_{i-\frac{1}{2},j} + \overline{V}_{i,j+\frac{1}{2}} - \overline{V}_{i,j-\frac{1}{2}}\Big]\,, \tag{16}$$

where $\Delta\mathscr{A}_{i,j}$ is the horizontal area of the grid box i, j;

$$\overline{U}_{i+\frac{1}{2},j} = \sum_{k=1}^{N} U_{i+\frac{1}{2},j,k}\,, \qquad \overline{V}_{i,j+\frac{1}{2}} = \sum_{k=1}^{N} V_{i,j+\frac{1}{2},j}\,, \tag{17}$$

are vertically integrated (barotropic) volume fluxes; and we have used the identity

$$\left(\zeta_{i,j}+h_{i,j}\right)\cdot\Delta\mathscr{A}_{i,j}\equiv\sum_{k=1}^{N}\Delta\mathscr{V}_{i,j,k}\,, \tag{18}$$

where $h_{i,j}$ is independent of time. Setting $k=N$ in (15), consistently with (16)–(18) results in

$$W_{i,j,N+\frac{1}{2}}=0\,, \tag{19}$$

as required by the kinematic boundary condition at the free surface.

Thus far it has been assumed that the time step and time-stepping algorithm for the tracer (10) and for ζ (16) are the same. This would be the case if the barotropic and baroclinic components were advanced using the same small time step dictated by the stability criterion for the barotropic mode. In a split-explicit, free-surface model, the equation for free-surface (16) and the vertically integrated (2D) momenta are advanced using a much smaller time step than the tracer equations. Each baroclinic time step starts with computation of the right hand side of the 3D momentum equations. The right hand side components are integrated vertically to provide forcing terms for the barotropic mode. During the barotropic time-stepping, the free surface and the barotropic velocity components are advanced with the short time step, then averaged over the sequence of the barotropic steps to prevent aliasing. Then the 3D momenta are advanced to the baroclinic time step $n+1$, and vertical integrals of the new fields are subtracted from the similar values from the barotropic submodel. The resultant differences are then uniformly distributed throughout the vertical column to make sure that the corrected 3D velocity components have the same vertical integrals as the barotropic ones. At the same time, the free surface ζ at the new baroclinic step is assigned its new value from the barotropic submodel.

Because of the replacement of ζ at $n+1$ with its fast-time-averaged value, it is no longer possible to reconstruct the vertical velocity via (15) in such a way that the top kinematic boundary condition (19) is respected. Alternatively on might distribute the mismatch in (19) throughout the water column, so that the top boundary condition holds, but at the expense of a discrepancy in (15), Song and Haidvogel (1994). In either case, a conservative update of the tracer fields (10) loses its constancy preservation property.

3.2 Mode-splitting error

In the split-explicit method, the shallow water equations (SWE) are advanced in time, using the smaller CFL-limited time step, to obtain the depth-integrated mode, *e.g.*,

$$\frac{\partial\overline{U}}{\partial t}+\ldots=-gD\nabla_x\zeta+\left\{gD\nabla_x\zeta+\mathscr{F}\right\}. \tag{20}$$

Here, g is the acceleration of gravity; $D=h+\zeta$ is total depth; $\overline{U}\equiv D\overline{u}$ is depth-integrated velocity (barotropic mass flux); $\nabla_x\zeta$ is a shorthand for $\partial\zeta/\partial x$; and

$$\mathscr{F}=-\frac{1}{\rho_0}\int_{-h}^{\zeta}\frac{\partial P}{\partial x}dz \tag{21}$$

is the vertically integrated pressure gradient. The latter is a functional of the topography, free-surface gradient, and free surface itself, as well as the vertical distribution of density and its gradient,

$$\mathscr{F}=\mathscr{F}\left[\nabla_x\zeta,\ \zeta,\ \nabla_x\rho(z),\ \rho(z)\right]. \tag{22}$$

The term in curly brackets in (20) is interpreted as barotropic-baroclinic mode coupling. It is kept "frozen" during the barotropic time-stepping while the first term on the right side evolves. The disadvantage of this approach is that after the barotropic time-stepping is complete and the new free-surface field is substituted into

the full baroclinic pressure gradient, its vertical integral will no longer be equal to the sum of the SWE-like pressure gradient (computed using the new free surface) and the original coupling term (based on the old free surface). This is usually known as *mode-splitting* error.

Unfortunately, this error plays the role of a disturbance, causing the vertically integrated pressure gradient to be not in equilibrium with the barotropic mass flux. The barotropic time-stepping drives the barotropic part toward an equilibrium, but it is disturbed again due to the redefinition of the vertically integrated baroclinic pressure gradient. Higdon and Bennett (1996) analyzed the stability of a coupled linearized system in an isopycnic vertical coordinate and showed that, if non-dissipative time-stepping algorithms are used for both modes, the resultant model is unavoidably unstable. An alternative definition of the barotropic mode in an isopycnic model that reduces the mode splitting error is obtained by replacing both $gD\nabla_x\zeta$ terms in (20) with

$$\frac{\partial \mathscr{F}}{\partial (\nabla_x \zeta)} \nabla_x \zeta + \frac{\partial \mathscr{F}}{\partial \zeta} \zeta \, . \tag{23}$$

This replacement may be shown to remove the dominant mode splitting error.

4 ROMS split-explicit time-stepping algorithm

The redesigned time-stepping used in ROMS introduces several new features, including:

- forward-backward feedback between the pairs of variables responsible for gravity wave propagation (surface or internal) that combine an extended range of stability with the temporal accuracy of the best known algorithms, in effect, generalizing traditional forward-backward schemes to higher orders of accuracy;
- redefinition of the barotropic mode equations to account for the non-uniform density field to reduce mode-splitting error;
- a temporal weighted-averaging of the barotropic mode that allows an accurate representation of the barotropic motions resolved by the baroclinic time step (*e.g.*, tides and barotropic Rossby waves); and
- simultaneous conservation and constancy preservation properties for tracers in the evolving coordinate system due to changes in ζ.

We next give brief details on the last three of these algorithmic improvements, referring the reader to Shchepetkin and McWilliams (2004) for a full description of the new split-explicit method and its properties.

4.1 Improved mode-splitting

The algorithms in ROMS take into account the effects of the non-uniform density field, resulting in a more accurate mode-splitting method that is suitable for use in a terrain-following model. Consider a fluid element bounded horizontally by two vertical lines corresponding to the locations of ζ_i and ζ_{i+1} and vertically by the free surface and bottom (Fig. 1, left). The horizontal component of the pressure-gradient force acting on this element is calculated by the integration of the pressure along the contour surrounding the fluid element:

$$F_{i+\frac{1}{2}} = \int_{-h_i}^{\zeta_i} P(x_i, z)\, dz - \int_{-h_{i+1}}^{\zeta_{i+1}} P(x_{i+1}, z)\, dz - \int_{x_i}^{x_{i+1}} P\,(x, -h(x))\, \left[-\frac{\partial h(x)}{\partial x} \right] dx = \mathscr{I}_i - \mathscr{I}_{i+1} - \mathscr{I}_{i+\frac{1}{2}} \, , \tag{24}$$

where the contribution of atmospheric pressure along the upper surface has been neglected. In (24) $P(x,z)$ is the hydrostatic pressure,

$$P(x,z) = g \int_{z'}^{\zeta_i} \rho(x,z')\, dz' \, . \tag{25}$$

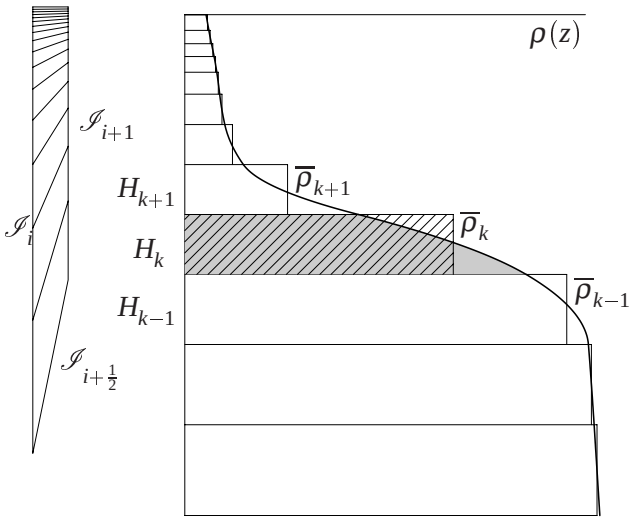

Figure 1: **Left:** *Fluid element showing placement of different terms in (24).* **Right:** *Reconstruction of the vertical density profile by parabolic segments (31): for each $k = 1,2,\ldots,N$, $\overline{\rho}_k$ are density averaged over grid boxes H_k of a vertically non-uniform grid. The shaded area is the same as the area of the diagonally hatched rectangle.*

Assuming a finite-volume approach to approximate (25) and eventually (24) at the discrete level, the barotropic pressure-gradient force at the velocity point $i+\frac{1}{2}$ is a function of the density in the vertical columns i and $i+1$, as well as the free-surface elevations ζ_i, ζ_{i+1}. Hence,

$$F_{i+\frac{1}{2}} = \mathscr{F}\left(\zeta_{i+1}, \overline{\rho}_{i+1,1}, \ldots, \overline{\rho}_{i+1,N}, \zeta_i, \overline{\rho}_{i,1}, \ldots, \overline{\rho}_{i,N}\right), \tag{26}$$

where the structure of the functional $\mathscr{F}$ depends upon the discretization details of the baroclinic pressure gradient, typically involving nonlinear interaction of $\zeta_{i'}$ and $\overline{\rho}_{i',k}$ fields.

In the ROMS mode-splitting technique, it is assumed that ζ is changing during the barotropic time-stepping while the density values, $\left\{\overline{\rho}_{i,k}\right\}$, remain frozen and change only during the baroclinic time step. However, the nonlinear relation (26) holds in barotropic time. Of course, it would be prohibitively inefficient to recompute $\mathscr{F}$ in (26) at every barotropic step by vertical integration of the whole 3D pressure gradient. Instead, in each vertical column, once at every baroclinic time step before the barotropic mode calculation begins, ROMS computes a vertically averaged density,

$$\overline{\rho}(x) = \frac{1}{D}\int_{-h(x)}^{\zeta(x)} \rho(x,z)dz, \tag{27}$$

and a vertically averaged dynamical density,

$$\rho^*(x) = \frac{1}{\frac{1}{2}D^2}\int_{-h(x)}^{\zeta(x)} \left\{\int_z^{\zeta(x)} \rho(x,z')dz'\right\} dz, \tag{28}$$

where $D \equiv D(x) = \zeta(x) + h(x)$ is the total thickness of the water column. Changing the integration variable to $\sigma = (z-\zeta)/D$ yields

$$\overline{\rho}(x) = \int_{-1}^{0} \rho(x,\sigma)d\sigma, \quad \rho^*(x) = 2\int_{-1}^{0} \left\{\int_{\sigma}^{0} \rho(x,\sigma')d\sigma'\right\} d\sigma,$$

which implies that $\overline{\rho}$ and ρ^* are actually independent of ζ as long as the density profile $\rho = \rho(\sigma)$ stays the same. Expressed in terms of $\overline{\rho}$ and ρ^*, (24) becomes

$$F_{i+\frac{1}{2}} = g\left\{\frac{\rho_i^* D_i^2}{2} - \frac{\rho_{i+1}^* D_{i+1}^2}{2} + \int_{x_i}^{x_{i+1}} \overline{\rho} D \frac{\partial h}{\partial x} dx\right\}. \tag{29}$$

This is a finite-volume discretization of the pressure-gradient term in the vertically integrated momentum equation,

$$\frac{\partial}{\partial t}\left(D\overline{U}\right) + \ldots = -\frac{1}{\rho_0} g\left\{\frac{\partial}{\partial x}\left(\frac{\rho^* D^2}{2}\right) - \overline{\rho} D \frac{\partial h}{\partial x}\right\} = -\frac{1}{\rho_0} gD\left\{\rho^* \frac{\partial \zeta}{\partial x} + \frac{D}{2}\frac{\partial \rho^*}{\partial x} + \left(\rho^* - \overline{\rho}\right)\frac{\partial h}{\partial x}\right\}. \tag{30}$$

If $\rho^* \equiv \overline{\rho} \equiv \rho_0$, the right side of (30) reverts back to the familiar SWE pressure-gradient term of (20), but in the general case non-uniformity of $\overline{\rho}$ and ρ^* leads to the appearance of two extra terms that are baroclinic in nature. The problem therefore reduces to the search for a suitable method of calculation of $\overline{\rho}$ and ρ^* from the 3D density field $\left\{\overline{\rho}_{i,k}\right\}$ and an appropriate discretization of (29)–(30).

To address the first issue, consider, *e.g.*, a piecewise-parabolic reconstruction of the vertical density profile from a set of discrete values $\left\{\overline{\rho}_k \,|\, k = 1, \ldots, N\right\}$ that is interpreted as a set of grid-box averages within each vertical vertical grid box H_k (Fig. 1),

$$\rho(z') = \overline{\rho}_k + \frac{\rho_{k+\frac{1}{2}} + \rho_{k-\frac{1}{2}}}{H_k} z' + 6\left(\frac{\rho_{k+\frac{1}{2}} + \rho_{k-\frac{1}{2}}}{2} - \overline{\rho}_k\right)\left[\frac{z'^2}{H_k^2} - \frac{1}{12}\right]. \tag{31}$$

Here the local vertical coordinate z' spans the grid box H_k, so that $-\frac{H_k}{2} \le z' \le +\frac{H_k}{2}$, and $\rho_{k\pm\frac{1}{2}} \equiv \rho\left(\pm\frac{H_k}{2}\right)$ are the density values at at the upper and lower grid box interfaces, $z = \pm\frac{H_k}{2}$ computed via an appropriate reconstruction algorithm. Regardless of the details of computing $\rho_{k\pm\frac{1}{2}}$, (31) guarantees that

$$\frac{1}{H_k}\int_{-H_k/2}^{+H_k/2} \rho(z')\, dz' \equiv \overline{\rho}_k \tag{32}$$

and leads to the discretization of vertically averaged density,

$$\overline{\rho}_i = \sum_{k=1}^{N} \overline{\rho}_{i,k} H_{i,k} \Bigg/ \sum_{k=1}^{N} H_{i,k}. \tag{33}$$

To compute ρ^* we note from (31)–(32) that the hydrostatic pressure in (24) can be expressed as a continuous function within each grid box H_k,

$$\begin{aligned} P(z') = P_{k+\frac{1}{2}} + g\int_{z'}^{H_k/2} \rho(z'')\, dz'' = P_{k+\frac{1}{2}} \\ + gH_k\left\{\overline{\rho}_k\left[\frac{1}{2} - \frac{z'}{H_k}\right] + \frac{\rho_{k+\frac{1}{2}} - \rho_{k-\frac{1}{2}}}{2}\left[\frac{1}{4} - \frac{z'^2}{H_k^2}\right]\right. \\ \left. + 2\left(\frac{\rho_{k+\frac{1}{2}} + \rho_{k-\frac{1}{2}}}{2} - \overline{\rho}_k\right)\left[\frac{z'}{4H_k} - \frac{z'^3}{H_k^3}\right]\right\}, \end{aligned} \tag{34}$$

where $P_{k+\frac{1}{2}}$ is the pressure at a depth corresponding to the interface between H_k and H_{k+1},

$$P_{N+\frac{1}{2}} = 0 \quad \text{and} \quad P_{k-\frac{1}{2}} = g\sum_{k'=k}^{N} \overline{\rho}_{k'} H_{k'}, \qquad k = 1, \ldots, N. \tag{35}$$

It can be verified from (34) that $P(-H_k/2) \equiv P_{k-\frac{1}{2}}$ and that the pressure distribution and its first derivative are continuous across the grid box interfaces.

Subsequent integration of (34)–(35) leads to

$$\mathscr{I}_i = \int_{-h_i}^{\zeta_i} P_i(z)\,dz = \sum_{k=1}^{N} \int_{-H_{i,k}/2}^{+H_{i,k}/2} P_i(z')\,dz' = \sum_{k=1}^{N} H_{i,k}\overline{P}_{i,k}, \tag{36}$$

where

$$\overline{P}_{i,k} = P_{i,k+\frac{1}{2}} + \frac{1}{2}gH_{i,k}\left(\overline{\rho}_{i,k} + \frac{\rho_{i,k+\frac{1}{2}} - \rho_{i,k-\frac{1}{2}}}{6}\right) = \frac{P_{i,k+\frac{1}{2}} + P_{i,k-\frac{1}{2}}}{2} + gH_{i,k}\frac{\rho_{i,k+\frac{1}{2}} - \rho_{i,k-\frac{1}{2}}}{12} \tag{37}$$

is the pressure averaged over $H_{i,k}$. This further leads to the definition of the vertically averaged dynamical density as

$$\rho_i^* = \frac{1}{\frac{1}{2}\left(\sum_{k=1}^{N} H_{i,k}\right)^2} \cdot \sum_{k=1}^{N} H_{i,k}\left[\left(\sum_{k'=k+1}^{N} \overline{\rho}_{i,k'}H_{i,k'}\right) + \frac{1}{2}H_{i,k}\left(\overline{\rho}_{i,k} + \frac{\rho_{i,k+\frac{1}{2}} - \rho_{i,k-\frac{1}{2}}}{6}\right)\right]. \tag{38}$$

Using the identity,

$$\sum_{k=1}^{N} H_{i,k}\left[\left(\sum_{k'=k+1}^{N} H_{i,k'}\right) + \frac{1}{2}H_{i,k}\right] \equiv \frac{1}{2}\left(\sum_{k=1}^{N} H_{i,k}\right)^2,$$

one can interpret (38) as just a weighted average. Furthermore, since

$$\sum_{k=1}^{N} H_{i,k} \equiv h_i + \zeta_i \equiv D_i, \tag{39}$$

(36) may be expressed as

$$\mathscr{I}_i = \frac{1}{2}g\rho_i^* D_i^2\,. \tag{40}$$

To approximate $\mathscr{I}_{i+\frac{1}{2}}$, we assume that D, $\overline{\rho}$, and h are linear functions of the horizontal coordinate between points x_i and x_{i+1}:

$$\begin{aligned}\mathscr{I}_{i+\frac{1}{2}} &= g\int_{x_i}^{x_{i+1}} \left(\overline{\rho}_i\frac{x_{i+1}-x'}{\Delta x} + \overline{\rho}_{i+1}\frac{x'-x_i}{\Delta x}\right)\left(D_i\frac{x_{i+1}-x'}{\Delta x} + D_{i+1}\frac{x'-x_i}{\Delta x}\right)\frac{h_{i+1}-h_i}{\Delta x}dx' \\ &= g\frac{\left(\overline{\rho}_i + \overline{\rho}_{i+1}\right)\left(D_i + D_{i+1}\right) + \overline{\rho}_i D_i + \overline{\rho}_{i+1}D_{i+1}}{6}\left(h_{i+1} - h_i\right).\end{aligned} \tag{41}$$

After some algebra, (40) and (41) yield

$$\begin{aligned}F_{i+\frac{1}{2}} = {} & g\frac{D_i + D_{i+1}}{2}\cdot\frac{\rho_i^* + \rho_{i+1}^*}{2}\left(\zeta_i - \zeta_{i+1}\right) \\ & + g\frac{D_i^2 + D_{i+1}^2}{4}\left(\rho_i^* - \rho_{i+1}^*\right) \\ & + g\frac{D_i + D_{i+1}}{2}\cdot\frac{\left(\rho_i^* - \overline{\rho}_i\right) + \left(\rho_{i+1}^* - \overline{\rho}_{i+1}\right)}{2}\left(h_i - h_{i+1}\right) \\ & + \frac{\left(\overline{\rho}_{i+1} - \overline{\rho}_i\right)\left(D_{i+1} - D_i\right)\left(h_{i+1} - h_i\right)}{12}.\end{aligned} \tag{42}$$

The terms on the first, second, and third lines are obviously similar to the first, second, and third terms on the right-hand-side of (30), respectively. The term on the fourth line in (42) is on the order of $\mathscr{O}\left((\Delta x)^3\right)$ while all three preceding terms are $\mathscr{O}(\Delta x)$, so the former is negligible relative to the others as $\Delta x \to 0$.

In the case of $\zeta_i = \zeta_{i+1} = 0$, hence $D_i = h_i$ and $D_{i+1} = h_{i+1}$, (42) becomes

$$F^{(0)}_{i+\frac{1}{2}} = g\left(\rho^*_i - \overline{\rho}_i\right)\frac{h_i^2}{2} - g\left(\rho^*_{i+1} - \overline{\rho}_{i+1}\right)\frac{h_{i+1}^2}{2} + g\left(\overline{\rho}_i - \overline{\rho}_{i+1}\right)\frac{h_i^2 + h_i h_{i+1} + h_{i+1}^2}{6}. \tag{43}$$

Unlike the SWE pressure gradient, this does not vanish unless there is a special balance between the densities ρ^*_i, ρ^*_{i+1}, $\overline{\rho}_i$, $\overline{\rho}_{i+1}$, and the unperturbed thicknesses, h_i and h_{i+1}. For example, if density is a linear function of depth, $\rho = \rho(z) = -\alpha z$ resulting in

$$\overline{\rho}_i = \frac{1}{h_i}\int_{-h_i}^{0}(-\alpha z)\,dz = \frac{\alpha h_i}{2} \tag{44}$$

$$\rho^*_i = \frac{2}{h_i^2}\int_{-h_i}^{0}\int_{z}^{0}(-\alpha z')\,dz' = \frac{\alpha h_i}{3}. \tag{45}$$

Then $F^{(0)}_{i+\frac{1}{2}}$ vanishes, as verified by direct substitution of these expressions into (43).

We therefore split (42) into

$$F_{i+\frac{1}{2}} = F^{(0)}_{i+\frac{1}{2}} + F'_{i+\frac{1}{2}}, \tag{46}$$

where

$$\begin{aligned} F'_{i+\frac{1}{2}} = -\frac{1}{2}g\Big\{ & \left(h_i + h_{i+1}\right)\left(\rho^*_{i+1}\zeta_{i+1} - \rho^*_i\zeta_i\right) + \rho^*_{i+1}\zeta^2_{i+1} - \rho^*_i\zeta^2_i \\ & + \left(h_{i+1} - h_i\right)\Big[\left(\rho^*_{i+1} - \overline{\rho}_{i+1}\right)\zeta_{i+1} + \left(\rho^*_i - \overline{\rho}_i\right)\zeta_i \\ & + \frac{1}{3}\left(\overline{\rho}_{i+1} - \overline{\rho}_i\right)\left(\zeta_{i+1} - \zeta_i\right)\Big]\Big\} \end{aligned} \tag{47}$$

contains all the terms of (42) with ζ. The transition from (42) to (43)–(47) has no approximations.

If the density field is a function only of depth, the baroclinic pressure gradient should vanish. However, in order to make $F^{(0)}_{i+\frac{1}{2}} = 0$ in (43), there must be cancellation between its terms that can be achieved only by having a special relation between ρ^*_i and $\overline{\rho}_i$. Except for a few special choices of the density profile (constant, linear, or quadratic in z), this cancellation is not exact, but rather relies on the numerical accuracy of the integration method. This is often referred to as *hydrostatic inconsistency*. The use of a high-order integration method can reduce, but not totally eliminate, this error.

4.2 Temporal averaging of the barotropic mode

The requirements on the barotropic sub-model are to compute (i) $\langle\zeta\rangle^{n+1}$ and $\langle\overline{\mathbf{U}}\rangle^{n+1}$ at the new baroclinic time step $n+1$, properly averaged to filter out and avoid aliasing of barotropic time scales not resolved by the baroclinic time step, and (ii) the barotropic mass flux, $\langle\langle\overline{\mathbf{U}}\rangle\rangle^{n+\frac{1}{2}}$, integrated over the barotropic time steps, satisfying the slow-time, free-surface equation (16).

To fulfill task (i), choose an appropriate weighting shape function $\{q_m\}$ (Fig. 2, top panel) that satisfies discrete normalization and centroid conditions,

$$\sum_{m=1}^{M^*} a_m \equiv 1, \qquad \sum_{m=1}^{M^*} a_m \frac{m}{M} \equiv 1\ . \tag{48}$$

Here M denotes the barotropic-baroclinic mode-splitting ratio; *i.e.*, it takes M barotropic steps to advance the barotropic mode for the time interval corresponding to one baroclinic step. M^* is the last index at which $a_m \neq 0$, where $M \leq M^*$ to ensure that $\{a_m\}$ is time centered at $n+1$. Once $\{a_m\}$ is specified, we define the slow-time quantities (denoted by angle brackets),

$$\langle \zeta \rangle_{i,j}^{n+1} = \sum_{m=1}^{M^*} a_m \zeta_{i,j}^m \qquad \langle \overline{U} \rangle_{i+\frac{1}{2},j}^{n+1} = \sum_{m=1}^{M^*} a_m \overline{U}_{i+\frac{1}{2},j}^m \qquad \langle \overline{V} \rangle_{i,j+\frac{1}{2}}^{n+1} = \sum_{m=1}^{M^*} a_m \overline{V}_{i,j+\frac{1}{2}}^m , \tag{49}$$

where ζ^m, $\overline{U}^m$, and $\overline{V}^m$ are "instantaneous" barotropic variables. To satisfy the slow-time continuity equation (13), we have to construct another set of fast-time-averaged barotropic fluxes, $\langle\langle \overline{U} \rangle\rangle^{n+\frac{1}{2}}$ and $\langle\langle \overline{V} \rangle\rangle^{n+\frac{1}{2}}$, which are consistent with the change in sea level between the two consecutive slow-time steps,

$$\langle \zeta \rangle_{i,j}^{n+1} = \langle \zeta \rangle_{i,j}^{n} - \Delta t \cdot \mathrm{div} \langle\langle \overline{\mathbf{U}} \rangle\rangle_{i,j}^{n+\frac{1}{2}} \ . \tag{50}$$

This may be accomplished by the definition of a second set of weights, such that

$$\langle\langle \overline{U} \rangle\rangle_{i+\frac{1}{2},j}^{n+\frac{1}{2}} = \sum_{m=1}^{M^*} b_m \overline{U}_{i+\frac{1}{2},j}^{m-\frac{1}{2}} \qquad \langle\langle \overline{V} \rangle\rangle_{i,j+\frac{1}{2}}^{n+\frac{1}{2}} = \sum_{m=1}^{M^*} b_m \overline{V}_{i,j+\frac{1}{2}}^{m-\frac{1}{2}} \ . \tag{51}$$

As shown in Shcheptekin and McWilliams (2004), once $\{a_m\}$ is chosen, the other set $\{b_m\}$ may be uniquely determined.

4.3 Time Stepping the Coupled Baroclinic-Barotropic System

The ROMS time-stepping algorithm is designed to produce mutually consistent estimates of the new location of the sea surface (ζ^{n+1}), the associated barotropic mass fluxes ($\langle\langle \overline{\mathbf{U}} \rangle\rangle^{n+\frac{1}{2}}$), and the time-rates-of-change of the baroclinic fields (momentum and tracers) at time level $n+\frac{1}{2}$. Hence, the continuity equation on the long-time step (16) is satisfied and constancy preservation is assured. The time-stepping algorithm proceeds as follows (Fig. 2).

Stage 1: Compute the right side for the 3D momentum equations at time step n. Apply this right side to advance the 3D momenta using a Leapfrog (LF) step combined with a half-step, backward interpolation with Adams-Moulton (AM3-like) coefficients (the result is time-centered at $n+\frac{1}{2}$). Because no meaningful barotropic mass fluxes time-centered at $n+\frac{1}{2}$ are available yet, set the vertical averages for the newly computed fluxes back to $\langle \overline{\mathbf{U}} \rangle^n$.

Stage 2: Advance the tracer variables in a similar manner with a LF step combined with an AM3 interpolation, placing the resultant values at $n+\frac{1}{2}$.

Stage 3: Compute the right side for the 3D momentum equations from the mass fluxes and tracers (via density) at $n+\frac{1}{2}$. Vertically integrate everything and also compute and store vertically averaged densities, $\overline{\rho}$,ρ_i^*, using (33)-(38) time-centered at $n+\frac{1}{2}$. Apply the right side to the 3D momentum variables, but do not finalize the time step since H^{n+1} and $\langle \overline{\mathbf{U}} \rangle^{n+1}$ are not available yet.

Stage 4: Compute the right side terms for the barotropic mode from barotropic variables using (47) for the pressure gradient and subtract it from the corresponding vertical integrals of the 3D right side computed in Stage 3 (*i.e.*, convert them into baroclinic-to-barotropic forcing terms). Advance the barotropic variables (slightly beyond the baroclinic time step $n+1$, depending on the shape of the fast-time filter), performing a 2-way, fast-time averaging of barotropic variables on the way. The baroclinic forcing terms are kept constant during this procedure, but the barotropic pressure-gradient terms are recomputed by (47) with participation of $\overline{\rho}_i$ and ρ_i^* at every barotropic step. Once this is complete, update the vertical coordinate system, $\left\{ z_{i,j,k},\, z_{i,j,k+\frac{1}{2}},\, H_{i,j,k} \right\}^{n+1}$, to be consistent with $\langle \zeta \rangle^{n+1}$.

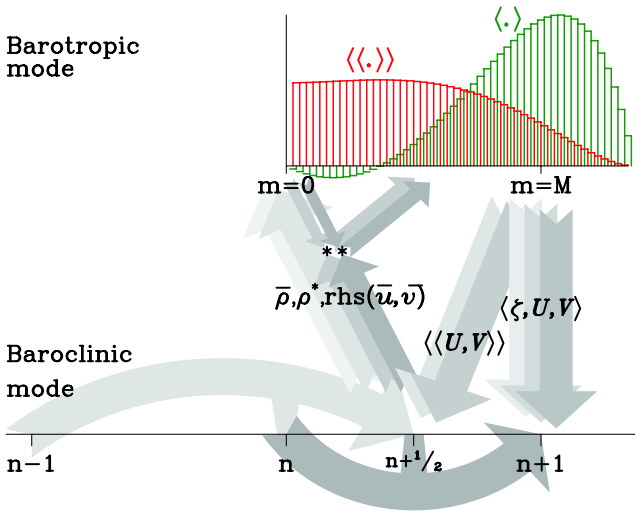

*Figure 2: Barotropic-baroclinic mode data exchange in ROMS: Curved horizontal arrows symbolize the predictor LF step combined with AM3 half-step-back interpolation of the result (light shading) and corrector sub-steps (dark shading). The four ascending arrows denote the 2-way, vertically averaged densities, $\overline{\rho}$ and ρ^*, and the vertically integrated right side for 3D momentum equations [the last two meet with the two small arrows symbolizing computation of the barotropic mode right hand side from barotropic variables; so that asterisks (*** ***) denote the computation of baroclinic-to-barotropic forcing terms, two small arrows ascending to the right]. The five large descending arrows symbolize 2-way, fast-time-averaged barotropic variables for backward coupling. Shown in the top panel are schematics of the barotropic temporal averaging weights a_m and b_m.*

Stage 5: Finalize the computation of the 3D mass fluxes begun in Stage 3 using the now available H^{n+1}, and set the vertical average to $\langle\overline{\mathbf{U}}\rangle^{n+1}$ from the barotropic mode.

Stage 6: Interpolate the 3D velocity components back in time to $n+\frac{1}{2}$ using a combination of the new time-step values (from Stage 5), values from the predictor step (Stage 4), and old-time step values. Set the vertical average of the resultant fields to $\langle\langle\overline{\mathbf{U}}\rangle\rangle^{n+\frac{1}{2}}$. Use the resultant velocity field and tracers at $n+\frac{1}{2}$ to compute the tracer fluxes and advance the tracers to $n+1$. This step is both conservative and constancy preserving.

Acknowledgements

The development and application of the ROMS model has been supported by grants from the Office of Naval Research (Ocean Modeling and Prediction), the National Science Foundation (NSF/ITR), the National Ocean Partnership Program (NOPP), the National Oceanic and Atmospheric Administration (NOAA), and the National Aeronautics and Space Administration (NASA).

References

Higdon, R. L. and A. F. Bennett, 1996. Stability analysis of operator splitting for large-scale ocean modelling. *J. Comp. Phys.*, **123**, 31–53.

Marchesiello, P., J. C. McWilliams, and A. F. Shchepetkin, 2001. Open boundary conditions for long-term integration of regional oceanic models. *Ocean Modelling*, **3**, 1–20.

Moore, A. M., H. G. Arango, E. Di Lornzo, B. D. Cornuelle, A. J. Miller and D. J. Neilson, 2004. A comprehensive ocean prediction and analysis system based on the tangent linear and adjoint of a regional ocean model.

Ocean Modelling, **7**, 227-258.

Shchepetkin, A. F. and J. C. McWilliams, 1998. Quasi-monotone advection schemes based on explicit locally adaptive dissipation. *Mon. Weather Rev.*, **126**, 1541–1580.

Shchepetkin, A. F. and J. C. McWilliams, 2003. A method for computing horizontal pressure-gradient force in an oceanic model with a nonaligned vertical coordinate. *J. Geophys. Res.*, **108**, 3090, doi:10.1029/2001JC001047.

Shchepetkin, A. F. and J. C. McWilliams, 2004. The Regional Ocean Modeling System (ROMS): A split-explicit, free-surface, topography-following-coordinate oceanic model. *Ocean Modelling*, in press.

Song, Y. T. and D. B. Haidvogel, 1994. A semi-implicit ocean circulation model using a generalized topography-following coordinate. *J. Comp. Phys.*, **115**, 228–248.

Warner, J. C., C. R. Sherwood, H. G. Arango and R. P. Signell, 2005. Performance of four turbulence closure models implemented using a generic length scale method. *Ocean Modelling*, **8**, 81–113.